Fisheries Research 201 (2018) 1–10

Contents lists available at ScienceDirect

Fisheries Research

journal homepage: www.elsevier.com/locate/fishres

Influence of oceanographic conditions on the distribution and abundance of blackfin tuna (*Thunnus atlanticus*) larvae in the Gulf of Mexico

Maëlle Cornic[a,*], Jay R. Rooker[a,b]

[a] Department of Marine Biology, Texas A&M University (Galveston Campus), 1001 Texas Clipper Road, Galveston, TX 77554, United States
[b] Department of Wildlife and Fisheries Sciences, Texas A&M University, College Station, TX 77843, United States

ARTICLE INFO

Handled by B Arara

Keywords:
Larvae
Generalized additive models
Oceanographic features

ABSTRACT

Information on early life history of economical important fisheries stocks are required to accurately estimate their population status. This study investigated blackfin tuna (*Thunnus atlanticus*) larvae distribution over six summers (2007–2011, 2015) in the northern Gulf of Mexico. Blackfin tuna were commonly observed and widely distributed in surface waters with frequency of occurrence ranging from 48% (2008) to 92% (2011). Inter-annual variability in density was observed with highest mean density recorded in 2009 (17.2 larvae 1000 m^{-3}) and lowest mean density in 2015 (2.2 larvae 1000 m^{-3}). Density also varied between months with higher overall mean density observed in July (9.2 larvae 1000 m^{-3}) compared to June (4.3 larvae 1000 m^{-3}). Generalized additive models (GAMs) based on presence/absence and density of blackfin tuna larvae determined that this species was present in areas of intermediate salinity (31–36) and higher sea surface temperature (SST > 29 °C). Blackfin tuna larvae were also strongly associated with convergent zones near the Loop Current and anticyclonic eddies. Environmental conditions deemed to be favorable from GAMs (salinity, SST and sea surface height) were combined with environmental data in 2011 and 2015 to predict the suitable habitat of blackfin tuna larvae from the outer continental shelf into oceanic waters (areas ≥100 m isobath). The amount of highly suitable habitat (> 10 larvae 1000 m^{-3}) in 2011 and 2015 varied between months (June 6%, July 51%); however, blackfin tuna larvae were predicted to occur at similar locations in surface waters along the continental slope and at the margin of the Loop Current. Overall, the results highlighted the importance of mesoscale features and oceanographic conditions on the distribution and abundance of blackfin tuna larvae.

1. Introduction

The Gulf of Mexico (GoM) supports highly productive commercial and recreational fisheries for tunas (Chesney et al., 2000). Due to overfishing, populations of yellowfin tuna (*Thunnus albacares*), bigeye tuna (*Thunnus obesus*) and Atlantic bluefin tuna (*Thunnus thynnus*) in this region are decreasing in abundance and are considered to be depleted or fully exploited (Majkowski, 2007; Juan-Jordá et al., 2011). Apart from these taxa, blackfin tuna (*Thunnus atlanticus*) is also an important component of the offshore tuna fishery in the GoM (NOAA, 2016), and despite the numerical dominance of blackfin tuna relative to other tunas, this species has received considerably less attention by the scientific community. Because directed commercial fisheries for tunas in the GoM and western Atlantic Ocean generally target bigeye, bluefin, and yellowfin tuna, the decline of these populations is expected to lead to an increase in fishing pressure on blackfin tuna, which is troubling because no stock assessment or management plan currently exists for this species (ICCAT, 2016).

Understanding the population dynamics of blackfin and other tunas relies on accurate catch or abundance data as well as basic life history information (Fromentin and Fonteneau, 2001; Fromentin and Powers, 2005; Young et al., 2006). Stock abundance of tunas is often predicted using catch rates from a variety of sources (e.g., survey data, reported landings); however, using catch data to estimate key population parameters (e.g., spawning stock biomass) of tunas is problematic because these data are not necessarily reflective of population size, as they represent relative abundance of specific size in particular regions (Maunder et al., 2006). Because most of stock assessments of tunas are based on catch data, environmental and biological factors that affect the population dynamic are typically not integrated in assessment models, which can lead to inaccurately estimated trends in population size (Rouyer et al., 2008; Taylor et al., 2011). New analytical tools have been developed based on fishery-independent measure of abundance taking into account spatial and temporal distribution patterns of exploited species (Lehodey et al., 2003, Lamkin et al., 2015). In particular, larval abundance indices are often used as a proxy or indirect

* Corresponding author.
E-mail address: cornicm@tamug.edu (M. Cornic).

https://doi.org/10.1016/j.fishres.2017.12.015
Received 21 July 2017; Received in revised form 21 December 2017; Accepted 28 December 2017
Available online 09 January 2018
0165-7836/

means of predicting spawning stock biomass of tunas and other pelagic fishes (Scott et al., 1993; Hsieh et al., 2006; Ingram et al., 2017). Therefore, determining the influence of environmental conditions – both biotic and abiotic – on the spatial dynamics of blackfin tuna larvae is fundamental to assessing their population status.

Blackfin tuna stock status is uncertain in the GoM, as basic information on the spawning and early life habitat of blackfin tuna is limited for this region. Therefore, abundance estimates of blackfin tuna larvae in the GoM can provide critical information that can be used to assess stock status but also determine the timing and location of spawning in this region. It has been observed that potential environmental changes can impact the spatial and temporal dynamics of spawning areas, which influence the distribution and abundance of tuna larvae (Lindo-Atichati et al., 2012; Reglero et al., 2014). The northern GoM has been described as an essential spawning and nursery habitat of blackfin tuna (Rooker et al., 2013; Cornic et al., 2018), and the distribution and abundance of tuna larvae has been related to seasonal variations in the geographic position of the Loop Current and physicochemical conditions associated with this feature (Lindo-Atichati et al., 2012; Muhling et al., 2013). Due to the fact that physicochemical conditions of a nursery habitat are known to influence the growth and survival of tuna larvae (García et al., 2013; Kim et al., 2015), it can be expected that oceanographic features associated with early life habitats of blackfin tuna will affect their growth, survival, and recruitment. Therefore, defining environmental factors associated with early life habitats and the location of putative production zones for blackfin tuna is essential to understanding the influential drivers of recruitment success for this species in the GoM.

The objective of this study was to characterize the spatiotemporal patterns in distribution and abundance of blackfin tuna larvae in surface waters of the northern GoM. Because the distribution and abundance of tuna larvae depend on environmental factors of their habitat, generalized additive models (GAMs) based on presence-absence (P/A) and density were developed to determine the most influential environmental parameters affecting blackfin tuna larvae. Explanatory variables from GAMs were used to predict the distribution of blackfin tuna larvae based on environmental conditions in 2011 and 2015, and the estimated probabilities were then used to characterize the spatial extent and areal coverage of suitable habitats of blackfin tuna larvae in each year.

2. Materials and methods

2.1. Sampling protocol

The Gulf of Mexico (GoM) is semi enclosed sea, and oceanographic conditions off its continental shelf are generally oligotrophic and influenced by the Loop Current, a warm surface waters moving from the Caribbean Sea to the Atlantic Ocean through the GoM and the Florida Strait (Fig. 1). The Loop Current expansion in the GoM is highly variable and generates anticyclonic and cyclonic eddies that can affect the sea surface temperature and productivity of its region (Muller-Karger et al., 2015). Apart from the Loop Current, the northern GoM is influenced by seasonal riverine discharges from the Mississippi River that can modify the physicochemical characteristics (i.e salinity, turbidity) and productivity on the continental shelf and slope (Dagg et al., 2004).

Ichthyoplankton surveys were performed in June and July from 2007 to 2011 and 2015 in the northern GoM (Fig. 1). Blackfin tuna were collected in surface waters using neuston nets (1 m × 2 m frame) with 80% of the mouth of the net below the water. Therefore, larval densities were calculated under the assumption that neuston nets sampled at an average depth of 0.8m. From 2007–2010 two neuston nets with different mesh sizes (500 and 1200 μm) were used, while only one neuston net (1200 μm) was deployed in 2011 and 2015. Nets were deployed during the day for a duration of 10 min at an approximate speed of 1 ms^{-1}, with deployments being made every 15 km in order to sample diverse oceanographic features. Each net was equipped at its center with a General Oceanic flowmeter (Model 2030R, Miami, FL) to estimate the volume of water sampled. All fish larvae were fixed on board in 95% ethanol and later preserved in 70% ethanol.

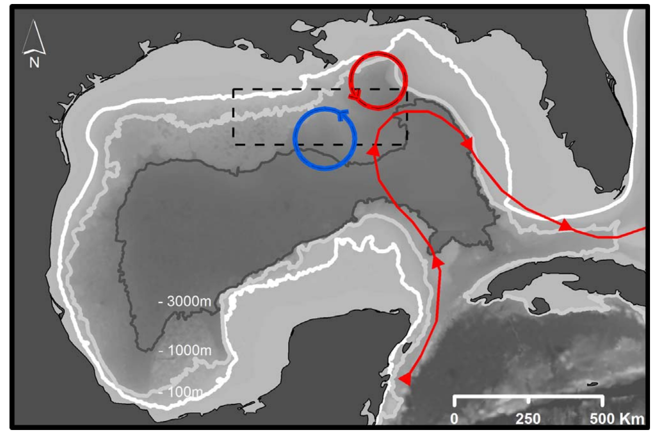

Fig. 1. Sampling area (dashed rectangle) of the June and July ichthyoplankton cruises performed from 2007 to 2011 and 2015 in the northern Gulf of Mexico. General oceanography of the Gulf of Mexico is represented by the Loop Current (red line), anticyclonic eddy (red circle), and cyclonic eddies (blue circle). (For interpretation of the references to colour in this figure legend, the reader is referred to the web version of this article.)

2.2. Environmental data

Sea surface temperature (SST, °C) and salinity were recorded at each sampling station (n = 325) from the research vessel using a Sonde 6920 Environmental Monitoring System (YSI Inc.). Also, *Sargassum* biomass (wet weight in kg) collected in neuston nets was recorded at each station. Additional environmental data at each station were extracted from open access resources using the Marine Geospatial Ecology Toolbox in ArcGIS (Roberts et al., 2010). Sea surface height anomaly (SSHA, cm) data were determined from remotely sensed data that matched our sampling dates and station locations. Sea surface height anomaly data were generated every 7 days (d) from combined satellite altimetry measurements using Jason-1 and 2, ENVISAT/ERS- 1 and 2, Geosat Follow-On and Topex/Poseidon inter- laced (AVISO). Sea surface chlorophyll *a* concentrations ($mg\,m^{-3}$) were accessed from NASA Ocean Color Group's Moderate Resolution Imaging Spectroradiometer (MODIS) on the Aqua satellite. Chlorophyll *a* concentration data consisted of 8 d averaged time periods with a 1/24° resolution. Water depth (m) at sampling stations was obtained from NOAA's NGDC U.S. Coastal Relief Model. To generate predicted suitable habitat of blackfin tuna larvae in June and July 2011 and 2015, environmental data (SSHA, SST, salinity) were extracted from remotely sensed observations using a grid of 0.0833°. SSHA were estimated from AVISO, while SST and salinity were extracted from the Gulf of Mexico Hybrid Coordinate Ocean Model (GoM-HYCOM) and added to U.S. Navy Coupled Ocean Data Assimilation (NCODA) system.

2.3. Larval identification

At the laboratory, *Thunnus* larvae were visually sorted using morphological characteristics and pigmentation (Richards, 2006). Because *Thunnus* larvae were abundant (n = 16986) in our samples, only positive stations (*Thunnus* present) containing more than 10 larvae were genetically identified. A subset of 6974 *Thunnus* larvae from 61% of the overall positive stations (n = 530) were selected across the main areas of our sampling corridor (27–28°N transect) and/or oceanographic features for each survey. Then, each larva was genetically identified to the species level using high-resolution melting analysis (HRMA), following the protocol described by Cornic et al. (2018). At stations with less than 100 *Thunnus* larvae collected during a cruise, all individuals were genetically identified; otherwise, 100 randomly selected individuals were genetically identified and the number of blackfin tuna larvae was extrapolated to the total number of *Thunnus* larvae collected at the particular station. Standard length (SL) measurements to the nearest 0.01 mm were taken for blackfin tuna larvae genetically identified from 2007 to 2010 ($>$ 80%) using image analysis software (Image Pro Plus 7).

2.4. Data analysis

Because sampling gear type can affect catch of *Thunnus* larvae (Habtes et al., 2014), linear regression analyses were performed to investigate the potential influence of different sampling gears on blackfin tuna larvae catchability. Linear regression analysis showed that densities of blackfin tuna larvae were significantly different between neuston nets with 500 and 1200 µm mesh sizes (log + 1(net 500) = 0.35 + 0.84*log + 1(net 1200); $p < 0.01$) for all paired stations sampled from 2007 to 2010. Densities of blackfin tuna larvae were higher in the neuston net with 500 µm mesh size (10.0 + 1.0 larvae 1000 m^{-3}) than the 1200 µm (2.6 + 0.3 larvae 1000 m^{-3}) (Fig. S1, A). However, a significant positive relationship in density ($p < 0.01$) was observed between nets, indicating that spatial variation in the distribution and abundance of blackfin tuna larvae across our sampling stations was similar between the nets with different mesh sizes. It is also important to note that *Thunnus* larvae are commonly present below surface waters (Habtes et al., 2014). Consequently, we compared densities of larvae found in the upper meter of the water column (neuston net, 1200 µm mesh size) to oblique, bongo tows (paired nets, mesh size 333 and 500 µm) from the surface to 100 m depth (Fig. S1 A, B) from 2011 to 2015. Density of blackfin tuna larvae was statistically similar between gears that sampled the surface (neuston tows: 3.7 + 0.6 larvae 1000 m^{-3}) and the water column to 100 m (oblique bongo tows: 3.5 + 0.3 larvae 1000 m^{-3}) (paired *t*-test, $p = 0.4$). A significant positive correlation ($p < 0.01$) between the density of blackfin tuna larvae in surface waters and at depth for each station was observed, indicating that surveys conducted in surface waters appear to serve as a useful proxy for characterizing the relative abundance of blackfin tuna larvae found in the water column or at depth.

Percent frequency of occurrence was calculated for each survey as the total number of stations containing blackfin tuna larvae divided by the total number of stations with *Thunnus* larvae identified with HRMA plus stations without any *Thunnus* larvae present. Because only a subset of stations could be analyzed with HRMA, other stations with positive catches of *Thunnus* larvae but not assayed with HRMA were not included in the total number of stations sampled.

Because density data violated the assumptions of normality and homogeneity of variances, non-parametric tests were carried out with R (R Development Core Team, 2015). The aligned rank transform (ART) for nonparametric factorial ANOVAs test was performed to compare densities among years and between months using the package ARTool (Wobbrock et al., 2011). Differences in factor levels of main effects were examined by using the post-hoc interaction analysis using the package phia (De Rosario-Martinez, 2015).

Spatio-temporal distribution of blackfin tuna larvae in the northern GoM was visualized using kernel density based on the densities observed at each positive station from 2007 to 2010. Because kernel density estimation can be influenced by a skewed statistical distribution of data (Carpentier and Flachaire, 2015), a log(x + 1) transformation was applied to larval density prior to calculation. Then, kernel density was estimated with a cell size of 0.01 and search radius of 0.8 in ArcGIS Spatial Analyst tool.

Generalized additive models (GAMs) were developed in R (R Development Core Team, 2015) to examine the influence of environmental conditions on the occurrence and density of blackfin tuna larvae. Generalized additive models as allow parametric fixed effects to be modeled non-parametrically using additive smoothing functions, and relax the assumptions of normality and linearity inherent in linear regression (Hastie and Tibshirani, 1990; Guisan et al., 2002). Models included a suite of environmental parameters (SST, salinity, SSH, depth, surface chlorophyll *a*, and *Sargassum* biomass standardized by kilogram per kilometer towed), spatial parameters (longitude, latitude), and temporal parameters (hour after the sunrise, year, month). Two different models with cubic regression spline and logarithm link function were built; presence/absence (P/A) model using binomial distribution and density model using a negative binomial distribution. Degree of freedom of regression splines was penalized with a maximum degree of freedom of 4 to avoid overfitting while estimating the model parameters. The goodness-of-fit of each model was examined using Akaike information criterion (AIC). Collinearity among variables was examined using Spearman's test and variance inflation factor (VIF). If variables were highly correlated ($\rho > 0.60$ and VIF > 5), separate GAMs were run with each collinear variable to determine their influence on P/A and density of blackfin tuna larvae. The variable included in the GAM that resulted in the lowest AIC value was kept in the initial model. For both P/A and density models, depth and latitude were collinear, therefore latitude was removed from the initial model. For each model, a backwards stepwise procedure based on minimizing AIC was used to select explanatory variables influencing the P/A and density of blackfin tuna larvae. Non-significant smoothed variables ($p > 0.05$) were removed one by one from the initial model unless their removal involved an increase of AIC value. Final models were selected based on lowest AIC values. To determine the importance of each variable in the final model, variables were removed one by one from the final model and the variation in percent deviance explained (ΔDE) and AIC (ΔAIC) between the two models was calculated (Rooker et al., 2012).

Distribution maps of predicted densities were developed to determine the location of suitable habitat of blackfin tuna larvae in the GoM for 2011 and 2015. Because habitat quality of tuna larvae is influenced primarily by the oceanographic conditions (Muhling et al., 2013; Rooker et al., 2013; Reglero et al., 2014; Cornic, 2017), only the most influential physicochemical parameters (e.g., salinity, SST, SSHA) detected in the density based GAMs developed from 2007 to 2010 were used. Moreover, during the summer 2010 the northern GoM was affected by the Deepwater Horizon oil spill (Crone and Tolstoy, 2010) that potentially affected habitat conditions and the survival of blackfin tuna larvae (Rooker et al., 2013; Incardona et al., 2014). As a result, this year was removed from the analysis and blackfin tuna larvae densities were predicted in June and July 2011 and 2015 based on the three most influential explanatory variables from 2007 to 2009 (GAMs; Table S1; Fig. S2) using pred.gam function in the mgcv package in R (Wood, 2015). Then, predicted densities were smoothed using a bilinear interpolation and plotted in ArcGIS to visualize the distribution of blackfin tuna larvae from the 100-m isobath (depth contour) to the oceanic waters of the northern GoM (Rooker et al., 2013), and the percent coverage of highly suitable habitat ($>$ 10 larvae 1000 m^{-3}) was estimated.

Although P/A and density GAMs for blackfin tuna larvae were influenced by similar environmental parameters (SST, SSHA, salinity), the density based model represented a better fit of our data (AIC = 1840.4; DE = 36.6%), and was used to predict the habitat suitability of blackfin tuna larvae in 2011 and 2015 from the 100-m isobath into oceanic waters (Table S1; Fig. S2).

3. Results

3.1. Catch summary

An overall of 5687 blackfin tuna larvae were identified among six-sampling years. Standard length (SL) of 71% of the blackfin tuna larvae identified was recorded, and nearly all (99%) of the blackfin tuna larvae collected were less than 6 mm SL (mean = 4.6 mm SL) (Fig. 2). Blackfin

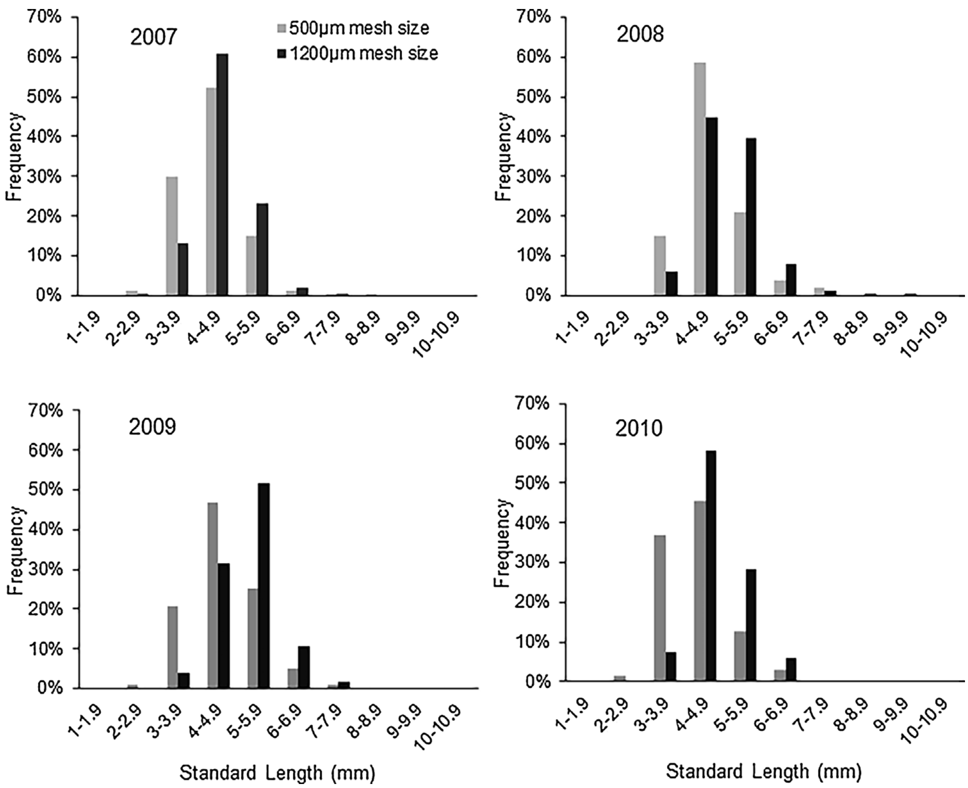

Fig. 2. Size distribution of blackfin tuna larvae (standard length, mm) from 2007 to 2010 in the northern Gulf of Mexico.

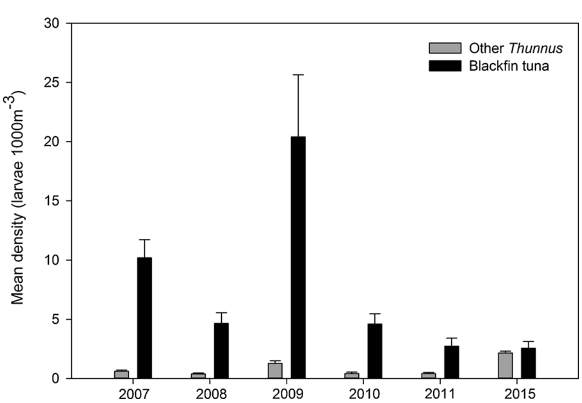

Fig. 3. Density (larvae 1000 m^{-3}) of blackfin tuna and other *Thunnus* larvae (bluefin tuna, yellowfin tuna, and bigeye tuna) in the northern GoM from 2007 to 2011 and 2015. Error bar represent one standard error of the mean.

Table 1
Summary of blackfin tuna larvae catches from 2007 to 2011 and 2015. n corresponds to the number of stations genetically analyzed, count is the number of blackfin tuna larvae identified, and% of blackfin tuna represents the percent of blackfin tuna larvae identified in the *Thunnus* larvae collection. Densities (larvae 1000m^{-3}) and standard error of the mean (SE) are also indicated.

Year	Cruises	n	Count	% blackfin tuna	Frequency of occurrence	Densities (SE)
2007	June	22	420	79	79	5.8 (1.8)
	July	22	659	89	92	13.5 (1.6)
2008	June	25	472	66	52	4.8 (1.7)
	July	24	531	88	43	4.6 (0.6)
2009	June	32	623	84	76	6.0 (1.1)
	July	34	1193	82	81	29.2 (5.7)
2010	June	28	316	63	62	3.7 (1.7)
	July	33	464	87	75	6.3 (0.6)
2011	June	23	407	85	87	4.1 (0.6)
	July	34	166	98	66	1.4 (0.2)
2015	June	25	167	72	50	1.8 (2.9)
	July	23	269	88	48	3.3 (1.4)

tuna larvae were the most common true tuna in our samples, accounting for 82% of the *Thunnus* larvae collected (n = 6947) in the ichthyoplankton surveys of surface waters in the northern GoM. Mean density of blackfin tuna larvae (6.7 larvae 1000 m^{-3}) was high relative to all other *Thunnus* spp. collected (mean density 1.2 larvae 1000 m^{-3}) (Fig. 3). Percent frequency of occurrence for blackfin tuna larvae ranged from a low of 48% (2008) to a high of 92% (2011) (Table 1). Densities of blackfin tuna larvae varied significantly among years (ART test; $p < 0.01$), with mean values ranging from 2.5 larvae 1000 m^{-3} (2015) to 17.6 larvae per 1000 m^{-3} (2009) (Table 1; Fig. 3). A month effect was also observed with overall mean densities lower in June cruises (4.3 larvae 1000 m^{-3}) than July cruises (9.2 larvae 1000 m^{-3}) (ART test; $p < 0.01$). However, a year × month interaction effect was also detected (ART test; $p < 0.05$) with significantly higher blackfin tuna larval densities observed in June for 2008 and 2011, indicating that intra-annual differences were not consistent across all sampling years.

Blackfin tuna larvae were widely distributed throughout the sampling area in the northern GoM (Fig. 4); nevertheless, densities of blackfin tuna larvae were typically higher on the outer shelf and upper slope (depth ca. 200–2000 m) relative to more oceanic waters (> 2000 m depth). Moreover, different oceanographic features (anticyclonic eddy and the Loop Current) were present in our sampling corridor from 2007 to 2010, and a high number of blackfin tuna larvae (> 70%) were observed at the margin of the eddy (2007) and the Loop Current (2008 and 2009), suggesting that oceanographic features influence the distribution of blackfin tuna larvae.

3.2. Habitat relationships

The final P/A based GAM included 5 variables: hour after the sunrise, SSHA, SST, salinity, and *Sargassum* biomass (Fig. 5). The final model AIC and deviance explained were 389.5 and 15.1%. Occurrence of blackfin tuna larvae in the northern GoM were significantly affected

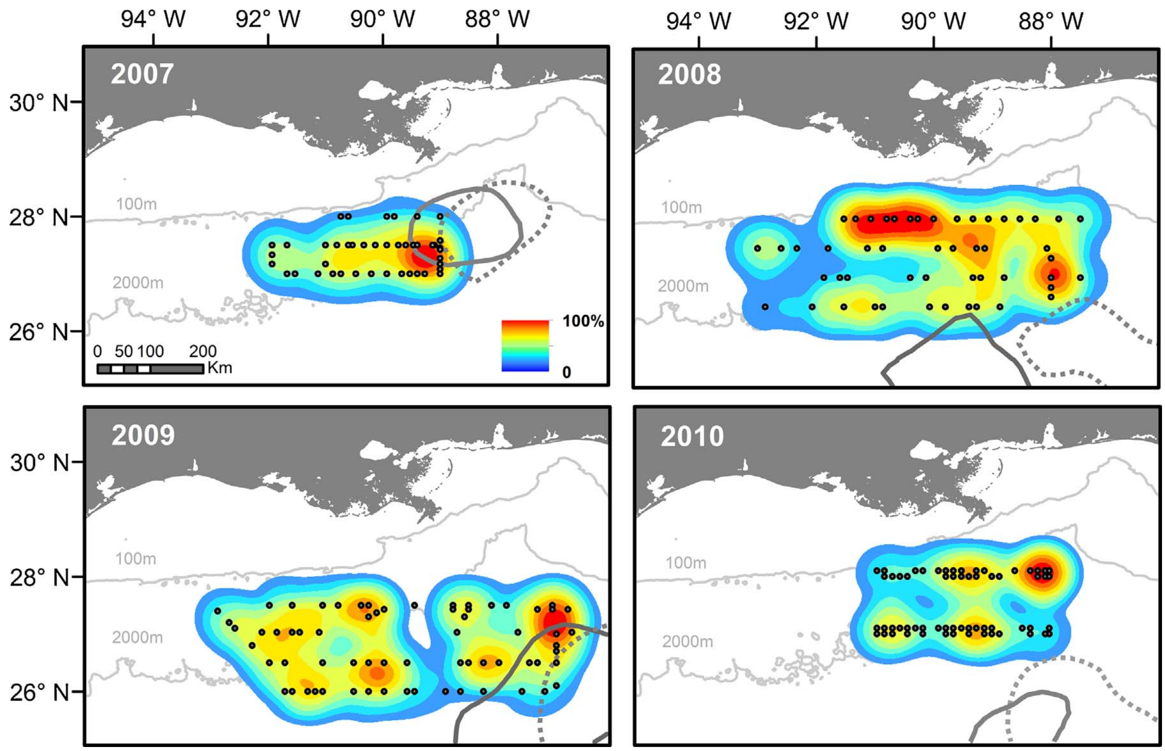

Fig. 4. Spatial distribution of blackfin tuna larvae from 2007 to 2010 in the northern Gulf of Mexico. Region corresponds to the sampling corridor represented in Fig. 1 (black rectangle). Black dots symbolize the stations genetically identified where blackfin tuna larvae were detected (June and July). Contour of kernel logarithm +1 transformed density (larvae 1000 m^{-3}) represent 20–100% of the total distribution of larvae. Grey lines represent the location of the Loop Current and anticyclonic features in June (dashed line) and July (plain line).

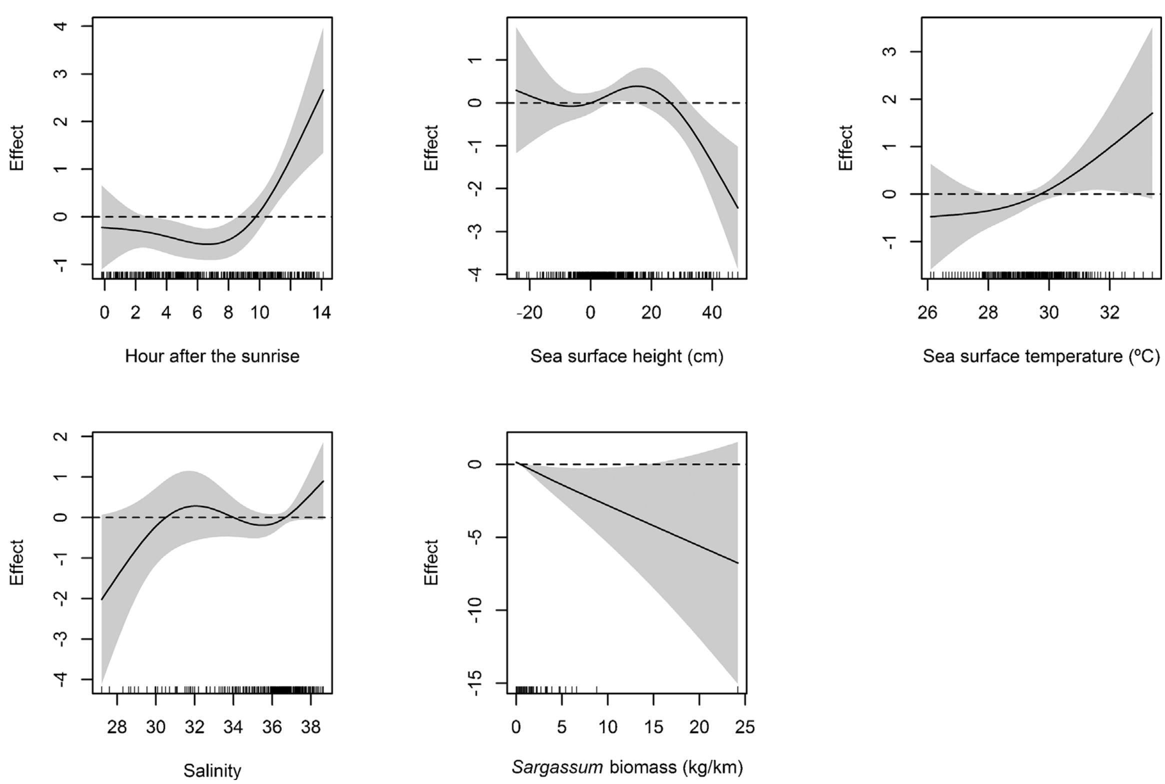

Fig. 5. Response plots from final generalized additive models (GAMs) showing the influence of environmental variables on presence-absence of blackfin tuna larvae from 2007 to 2010 in the northern Gulf of Mexico. On x-axis environmental variables and rug plot indicate number of observations, on y-axis the response of the model. Response curves are given by the solid lines and 95% confidence interval by the shaded areas.

Table 2
Variables retained in the final occurrence and density models, Akaike Information Criterion (AIC), deviance explained (DE).

Model	Variables	Δ AIC	Δ DE
Occurrence	Hour after sunrise***	22.1	7.3%
Final AIC: 389.5	SSHA*	8.1	3.5%
Final DE: 15.1%	SST	3.0	1.6%
	Salinity.	9.4	5.1%
	Sargassum biomass*	13.2	5%
Model	**Variables**	**Δ AIC**	**Δ DE**
Density	Year***	55	6.6%
Final AIC: 1840.4	Hour after sunrise***	33.3	4.3%
Final DE: 36.6%	SSHA***	32.0	4%
	SST***	36.2	4.7%
	Salinity***	15.1	2.3%
	Sargassum biomass**	9.8	1.3%

* $p < 0.05$.
** $p = 0.001$.
*** $p < 0.001$.

($p < 0.05$) by hour after the sunrise (ΔAIC = 22.1, ΔDE = 7.3%), SSHA (ΔAIC = 8.1, ΔDE = 3.5%), and *Sargassum* biomass (ΔAIC = 13.2, ΔDE = 5%) (Table 2), and response plots from final P/A based GAM showed that blackfin tuna larvae presence increased with both negative and positive SSHA (−10 to 20 cm), and at time periods > 10 h after the sunrise. In contrast, the larvae were negatively correlated with *Sargassum* biomass.

Results of the density based GAM were similar with 5 of the 6 variables also present in the P/A model (Fig. 6). Variables in the final density based GAM included: hour after the sunrise, SSHA, SST, salinity, *Sargassum* biomass, and year. Deviance explained (36.6%) was considerably higher than the P/A model and this model also resulted in a lower AIC (1840.4). Moreover, all the variables retained in the final density based model were significant ($p \leq 0.01$), with the most influential variables being year (ΔAIC = 55, ΔDE = 6.6%) and SST (ΔAIC = 36.6, ΔDE = 4.7%) (Table 2; Fig. 6). Densities were positively associated with negative and positive SSHA (−10 to 20 cm) (ΔAIC = 32, ΔDE = 4%), high SSTs (> 30 °C), intermediate to high salinity (> 30) (ΔAIC = 15.1, ΔDE = 2.3%) and period of the day > 10 h after the sunrise (ΔAIC = 33.3, ΔDE = 4.3%), while negatively correlated with *Sargassum* biomass (ΔAIC = 9.8, ΔDE = 1.3%).

3.3. Habitat suitability forecasting

Although P/A and density GAMs for blackfin tuna larvae were influenced by similar environmental parameters (SST, SSHA, salinity), the density based model represented a better fit of our data (AIC = 1840.4; DE = 36.6%), and was used to predict the habitat suitability of blackfin tuna larvae in 2011 and 2015 from the 100-m isobaths into oceanic waters. The resulting GAM was then related to the environmental data (SSHA, SST, and salinity) recorded in 2011 and 2015. Distribution maps of predicted densities indicated that blackfin tuna larvae were widely distributed in the northern GoM in 2011 and 2015, with higher densities observed on the edge of the predicted range along the 100 m (Fig. 7). Moreover, predicted densities of blackfin tuna larvae were highest (> 6 larvae 1000 m^{-3}) at the margin of Loop Current or associated warm core eddies as well as in areas of confluence between eddies. Areas with the lowest predicted densities occurred inside the Loop Current (0–0.2 larvae 1000 m^{-3}). Finally, distribution revealed that the availability of highly suitable habitat of blackfin tuna larvae (defined as predicted density of > 10 larvae 1000 m^{-3}) varied among month, with reduced spatial coverage in June (2% and 10%) relative to July (48% and 54%) (Table 3). Similar result was observed in the sampling corridor with no suitable habitat detected in June while 48% to 98% was detected in July 2011 and 2015, respectively.

4. Discussion

In the present study, both frequency of occurrence and density of blackfin tuna larvae in the surface waters of the northern GoM were high (82% and 6.7 larvae 1000^{-3}) relative to other *Thunnus* species

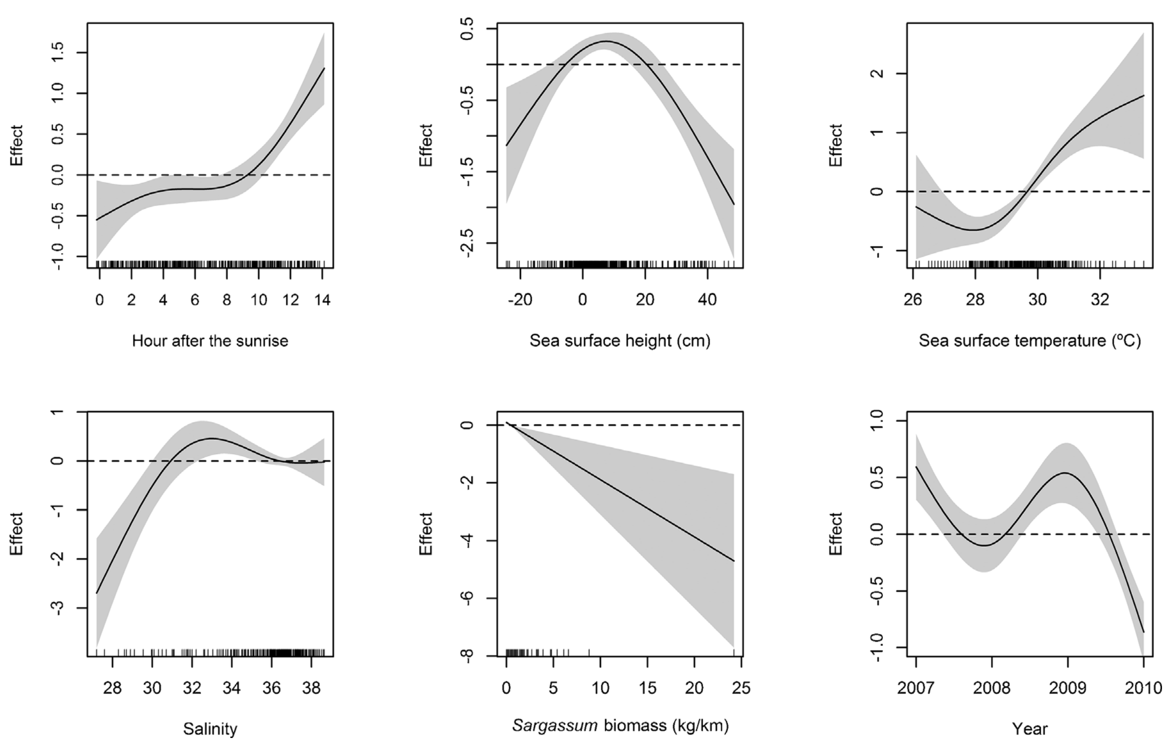

Fig. 6. Response plots from final generalized additive models (GAMs) showing the influence of environmental variables on density of blackfin tuna (larvae 1000 m^{-3}) from 2007 to 2010 in the northern Gulf of Mexico. On x-axis, environmental variables and rug plot indicate number of observations, on y-axis the response of the model. Response curves are given by the solid lines and 95% confidence interval by the shaded areas.

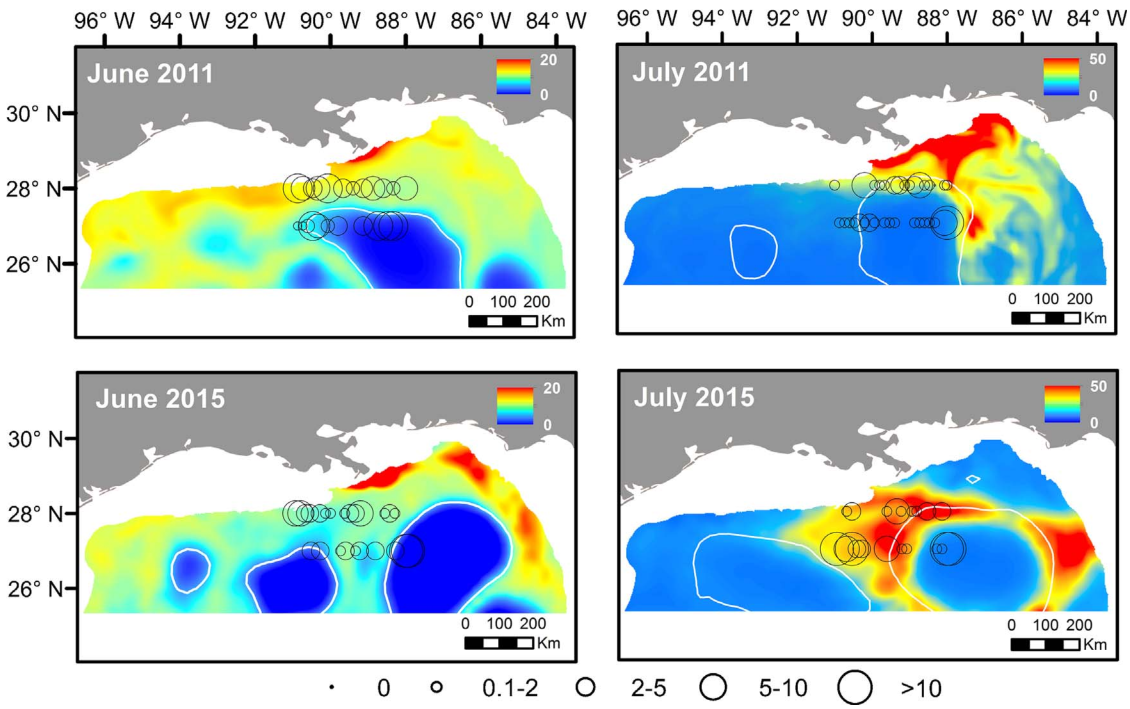

Fig. 7. Predictive maps of blackfin tuna larvae densities (larvae 1000 m^{-3}) developed based on density GAM models (2007–2009) and environmental conditions in June and July 2011 and 2015 in the northern Gulf of Mexico. White line indicates the location of the Loop Current and anticyclonic features, black circles symbolizes the densities observed during the ichthyoplankton cruises performed in this region in 2011 and 2015 (scale from 0 to > 10 larvae 1000 m^{-3}).

Table 3
Predicted area (km^2) and percent of highly suitable habitat (< 10 larvae 1000 m^{-3}) in the overall northern GoM and sampling corridor (black rectangle in Fig. 1).

Year	Month	Overall highly suitable habitat (km^2)	Overall percent of highly suitable habitat	Sampling corridor highly suitable habitat (km^2)	Sampling corridor percent of highly suitable habitat
2011	June	6378	2	0	0
	July	200536	48	15730	42
2015	June	44054	10	0	0
	July	227125	54	36695	98

(17–43% and 2.2 larvae 1000^{-3}), indicating that blackfin tuna larvae were the most common and abundant true tuna larvae in this region. Although growth rates for blackfin tuna larvae have not been established, the majority of blackfin larvae collected were relatively small (< 6 mm), and based on growth rates of other *Thunnus* larvae (Lang et al., 1994; Wexler et al., 2007) it appears that nearly all (ca. 99%) of the blackfin tuna larvae collected were within 10 days of hatching. This high abundance of small blackfin tuna larvae in June and July surveys indicates that spawning events likely occurred during both late spring and summer in the northern GoM. These results are consistent with other studies on early life ecology of tunas (Richardson et al., 2010; Rooker et al., 2013), supporting the premise that the GoM is an important spawning and nursery habitat for blackfin tuna.

Inter-annual variability in abundance is common for tuna larvae in the GoM as mesoscale features and oceanographic conditions are spatially and temporally dynamic (Muhling et al., 2010; Richardson et al., 2010; Rooker et al., 2013). While year was not retained in the P/A model, inter-annual variability in abundance was observed with mean densities ranging from 2.4 larvae 1000 m^{-3} to 17.6 larvae 1000 m^{-3} over six-sampling years. The spatial dynamics of the Loop Current are thought to be an important determinant of the temporal variability in abundance of tuna larvae (Lindo-Atichati et al., 2012; Cornic, 2017), as it alters environmental conditions in the northern GoM. Therefore, the penetration and spatial extent of the Loop Current likely affects the suitability of this region as nursery habitat for tuna larvae (Lindo-Atichati et al., 2012; Domingues et al., 2016). In 2009, high northward penetration of the Loop Current was linked to high densities of blackfin tuna larvae, which were observed at the margin of this mesoscale feature. In contrast, years of low Loop Current penetration (2008 and 2010) (Lindo-Atichati et al., 2013) corresponded to a decrease in densities for this species. Moreover, in 2010 the Deepwater Horizon event discharged large quantities of oil in the northern GoM, impacting large areas of potentially important early life habitat of tunas and other pelagic fishes (Crone and Tolstoy, 2010; Rooker et al., 2013). Because variability in larval abundance is often influenced by spatial and temporal differences in habitat quality (Lindo-Atichati et al., 2012), the degradation of spawning and nursery habitat of blackfin tuna in this region could have led the adults to spawn in other locations or led to an increase in larval mortality (Rooker et al., 2013; Incardona et al., 2014), which may be partly responsible for the reduced abundance of blackfin tuna larvae in 2010.

Spatial distribution patterns of tuna larvae have been related to the variability in physico-chemical conditions in the GoM (Muhling et al., 2013; Rooker et al., 2013; Cornic et al., 2018). Salinity was an important predictor of both distribution and abundance of blackfin tuna larvae, indicating that variation in salinity might affect the occurrence and survival of blackfin tuna larvae. In spring, freshwater discharge from the Mississippi River creates a salinity gradient from the Mississippi delta to the continental shelf in the northern GoM (Dagg et al., 2004). Blackfin tuna larvae were detected in a wide range of salinities; however, higher probability of occurrence and abundance were associated with intermediate salinities (30–34 psu), suggesting that marine areas impacted by freshwater inflow are potentially suitable habitat for blackfin tuna larvae. Furthermore, *Thunnus* larvae have a high metabolic demand for fast growth and increase prey availability often results in higher larval survival (Margulies, 1993; Tanaka et al., 2006). The increase of nutrients from riverine inputs influences primary and secondary production, increasing feeding opportunities for larval fish on the continental shelf of the northern GoM (Lohrenz et al., 1997).

Therefore, late spring and/or early summer spawning during riverine discharges may maximize the growth and survival of blackfin tuna larvae in this region.

Distribution and abundance of fish larvae in the GoM are heavily influenced by the location of mesoscale features such as Loop Current and associated eddies (Lindo-Atichati et al., 2012; Rooker et al., 2012). These features seasonally induce spatial variability in SST, with anti-cyclonic circulation features (warm-core eddies) characterized by nutrient-poor warm waters while cyclonic circulation features (cold-core eddies) are characterized by nutrient-rich colder waters. GAMs indicated that blackfin tuna larvae were well distributed across diverse water masses associated with different circulation features ($-10 < \text{SSHA} < 20$ cm), suggesting that this species has a high tolerance for varying environmental conditions. However, distribution and abundance of blackfin tuna larvae were positively associated with high SST (> 29 °C) and SSHA (> 10 cm), suggesting that the Loop Current and warm-core eddies might be more suitable habitat for this species compared to cold-core eddies. Tuna larvae are sensitive to temperature which can affect their growth and their ability to forage and avoid predators (Margulies, 1993; Wexler et al., 2011), and several studies have shown that warmer temperatures within anti-cyclonic features are favorable to blackfin tuna larvae (Richardson et al., 2010; Lindo-Atichati et al., 2012; Rooker et al., 2013). Moreover, frontal zones at the margin of the Loop Current and associated eddies can lead to the creation of convergent zones (Bakun, 2006), and our highest densities of blackfin tuna larvae were observed at or near convergence zones ($0 \text{ cm} < \text{SSHA} < 10$ cm). While physical forcing probably determines the distribution of blackfin tuna larvae within convergent zones (Bakun, 2006), it is also likely that increased feeding opportunities encountered in these zones will support growth and improve the survival of tuna larvae (Lamkin, 1997; Bakun, 2006; Govoni et al., 2010). Therefore, surface waters at the margin of the Loop Current and warm-core eddies may represent favorable habitat with optimal thermal conditions and prey resources for blackfin tuna larvae survival.

The spatial distribution of blackfin tuna is influenced by mesoscale features circulation that aggregate larvae and other external forcing factors (food availability, optimal sea surface temperature) (Richardson et al., 2010; Lindo-Atichati et al., 2012; Rooker et al., 2013). Suitable habitat for blackfin tuna larvae in our study was broadly dispersed along the continental slope (depth = 200–2000 m) in the north-central and eastern GoM, with the highest densities occurring near the margin of the Loop Current and areas of confluence between mesoscale features. Therefore, the presence of the Loop Current and other mesoscale features in northern GoM appears to influence the position and extent of highly suitable habitat available for blackfin tuna larvae. The geographical position of the Loop Current varied among years and seasons investigated. During 2011 and 2015 the northward penetration of this feature was higher in July and this may have contributed to the greater areal extent of highly suitable habitat observed for blackfin tuna in July than June. Consequently, the temporal variability in geographical location and shape of the Loop Current and associated features may affect the extent of suitable habitat for blackfin tuna which in turn, may influence the quality of their nursery habitat and their survival during the early life period. Also, it is important to note that high densities of blackfin tuna larvae were observed at the edge of our prediction range (100 m isobath), suggesting that the distribution of blackfin tuna larvae extends on the continental shelf or waters outside the prediction area.

Although differences in predicted and observed densities were detected for both years, the extent of the highly suitable habitat (> 10 larvae 1000m^{-3}) and the highest densities observed in our sampling corridor were similar, indicating that blackfin tuna larvae distribution based on predicted densities was valid to estimate their distribution and abundance in the northern GoM. The disparity between predicted and observed densities of blackfin tuna larvae was likely due to the fact that models were based on catch numbers from combined 500 and 1200 μm neuston net tows, while in 2011 and 2015, observed densities were calculated from a single 1200 μm mesh neuston net. Small larvae (< 4 mm SL) passing through the larger 1200 μm mesh size would result in lower overall density relative to estimates based on catches present in both 500 and 1200 μm mesh nets. In addition, it is also possible that shift in blackfin tuna larvae may be caused by environmental changes due to factors not included in our three-variable model that affected their distribution and abundance.

While this study focuses on a large spatial scale, small-scale vertical distribution can also affect the distribution and abundance of tuna larvae. Both distribution and abundance of blackfin tuna larvae varied during the day, with an increase in abundance at crepuscular periods prior to sunset and just after dawn. These results suggest that blackfin tuna larvae move to shallower depths in the water column at night. Vertical migrations are common in fish larvae and have been correlated to different factors such as light intensity, turbulence, predator avoidance, and prey concentration (Fortier and Harris, 1989; Job and Bellwood, 2000; Werner et al., 2001; Höffle et al., 2013). Vertical migrations of zooplankton are typically characterized by downward migrations during day and upward migrations at night to avoid predators (Dagg et al., 1989; Loose and Dawidowicz, 1994; Spinelli et al., 2015). Tuna larvae feed primarily on zooplankton (appendicularians, copepods and cladocerans) and other fish larvae (Llopiz et al., 2010), and by synchronizing their vertical migrations with those of their prey, blackfin tuna larvae may increase feeding opportunities. It is also important to note that the decrease of light intensity from sunset to sunrise may have also decreased the ability of larvae to avoid our towed nets. It has been observed that tuna catch can fluctuate between day/night and size of the larvae (Fortier and Harris, 1989; Davis et al., 1990; Boehlert and Mundy, 1994; Satoh et al., 2013; Habtes et al., 2014), which could have led to greater numbers of larvae caught at the end of the day. Diel differences in catch rates of blackfin tuna larvae in our study suggest that the vertical position of larvae or association with surface waters changes over time, which will have implications for their ecology as feeding, predation, and larval transport vary with depth (Boehlert and Mundy, 1994; Cowen and Sponaugle, 2009; Llopiz et al., 2010). Because our sampling was designed to sample larvae primarily associated with the upper 1 m of the water column (e.g, billfishes), future models that integrate the distribution of blackfin tuna at different depths within the water column as well as vertical profiles of key environmental parameters (e.g., sea surface temperature, prey biomass) will lead to improved predictive capabilities.

Spatial distribution and abundance of blackfin tuna larvae in surface waters of the northern GoM suggest that this region is an important spawning and nursery area for this species. Habitat associations of blackfin tuna larvae were influenced by specific physico-chemical conditions and the location of the Loop Current, suggesting that the margin of the Loop Current and convergence zones between mesoscale features are critical habitat for this species during early life. Results demonstrate the value of combined statistical models and GIS to predict the distribution of blackfin tuna larvae across large-scale features; however, further investigations on the influence of environmental conditions changes (e.g., water column depth, food availability) on this species would help to improve our understanding of habitat associations and population dynamics. Still, spatial and temporal patterns in habitat associations, distribution, and abundance presented here represent important baseline information, and these data can be used to develop accurate larval abundance indices to improve our understanding of the environmental conditions necessary for defining essential habitat as well as the timing of spawning for blackfin tuna in this region. Given the recent declines of true tunas in the Atlantic Ocean and associated basins such as the GoM, this information is essential to assess the population status of blackfin tunas as exploitation of this species may increase over the next decade.

Acknowledgements

A special thanks to members of the Fisheries Ecology and Fisheries Genetics labs for their assistance in the field and lab. Data are publicly available through the Gulf of Mexico Research Initiative Information & Data Cooperative (GRIIDC) at https://data.gulfresearchinitiative.org (doi: 10.7266/N7610XFM). This research was made possible by grants from the Gulf of Mexico Research Initiative (Deep Pelagic Nekton Dynamics consortium), the McDaniel Charitable Foundation, Louisiana State University, and the Louisiana Department of Wildlife and Fisheries.

Appendix A. Supplementary data

Supplementary data associated with this article can be found, in the online version, at https://doi.org/10.1016/j.fishres.2017.12.015.

References

Bakun, A., 2006. Fronts and eddies as key structures in the habitat of marine fish larvae: opportunity, adaptive response and competitive advantage. Sci. Mar. 105–122.

Boehlert, G.W., Mundy, B.C., 1994. Vertical and onshore-offshore distributional patterns of tuna larvae in relation to physical habitat. Ichthyol. Res. 55, 7–16.

Carpentier, A., Flachaire, E., 2015. Log-transform kernel density estimation of income distribution. L'Actual. Econ. Rev. Anal. Econ. 91, 141–159.

Chesney, E.J., Baltz, D.M., Thomas, R.G., 2000. Louisiana estuarine and coastal fisheries habitats: perspectives from a fish's eye view. Ecol. Appl. 10, 350–366.

Cornic, M., Smith, B.L., Kitchens, L.L., Alvarado Bremer, J.R., Rooker, J.R., 2018. Distribution and habitat associations of tuna larvae in the northern Gulf of Mexico. Hydrobiologia 806, 29–46.

Cowen, R.K., Sponaugle, S., 2009. Larval dispersal and marine population connectivity. Annu. Rev. Mar Sci. 1, 443–466.

Crone, T.J., Tolstoy, M., 2010. Magnitude of the 2010 gulf of Mexico oil leak. Science 330, 634–643.

Dagg, M.J., Frost, B.W., Walser, Jr.W.E., 1989. Copepod diel migration, feeding, and the vertical flux of pheopigments. Limnol. Oceanogr. 34, 1062–1071.

Dagg, M.J., Benner, R., Lohrenz, S., Lawrence, D., 2004. Transformation of dissolved and particulate materials on continental shelves influenced by large rivers: plume processes. Cont. Shelf Res. 24, 833–858.

Davis, T.L., Jenkins, G.P., Young, J.W., 1990. Diel patterns of vertical distribution in larvae of southern bluefin *Thunnus maccoyii*, and other tuna in the East Indian Ocean. Mar. Ecol. Prog. Ser. 59, 63–74.

De Rosario-Martinez, H., 2015. phia: post-hoc interaction analysis. R Package Version. pp. 1–3. (Available:). http://CRAN.R-project.org/package=phia.

Domingues, R., Goni, G., Bringas, F., Muhling, B., Lindo-Atichati, D., Walter, J., 2016. Variability of preferred environmental conditions for Atlantic bluefin tuna (*Thunnus thynnus*) larvae in the Gulf of Mexico during 1993–2011. Fish. Oceanogr. 25, 320–336.

Fortier, L., Harris, R.P., 1989. Optimal foraging and density-dependent competition in marine fish larvae. Mar. Ecol. Prog. Ser. 51, 19–33.

Fromentin, J.M., Fonteneau, A., 2001. Fishing effects and life history traits: a case-study comparing tropical versus temperate tunas. Fish Res. 53, 133–150.

Fromentin, J.M., Powers, J.E., 2005. Atlantic bluefin tuna: population dynamics, ecology, fisheries and management. Fish Fish. 6, 281–306.

García, A., Cortes, D., Quintanilla, J., Ramirez, T., Quintanilla, L., Rodriguez, J.M., Alemany, F., 2013. Climateinduced environmental conditions influencing interannual variability of Mediterranean bluefin (*Thunnus thynnus*) larval growth. Fish Oceanogr. 22, 273–287.

Govoni, J.J., Hare, J.A., Davenport, E.D., Chen, M.H., Marancik, K.E., 2010. Mesoscale, cyclonic eddies as larval fish habitat along the southeast United States shelf: a Lagrangian description of the zooplankton community. ICES J. Mar. Sci. 67, 403–411.

Guisan, A., Edwards, Jr.T.C., Hastie, T., 2002. Generalized Linear and Generalized Additive models in Studies of Species distributions: setting the scene. Ecol. Model. 157, 89100.

Habtes, S., Muller-Karger, F.E., Roffer, M., Lamkin, J.T., Muhling, B., 2014. A comparison of sampling methods for larvae of medium and large epipelagic fish species during spring SEAMAP ichthyoplankton surveys in the Gulf of Mexico. Limnol. Oceanogr. Methods 12, 86–101.

Hastie, T.J., Tibshirani, R.J., 1990. Generalized Additive Models, 1st Ed. Chapman and Hall, London.

Höffle, H., Nash, R.D.M., Falkenhaug, T., Munk, P., 2013. Differences in vertical and horizontal distribution of fish larvae and zooplankton related to hydrography. Mar. Biol. Res. 9, 629–644.

Hsieh, C.H., Reiss, C.S., Hunter, J.R., Beddington, J.R., May, R.M., Sugihara, G., 2006. Fishing elevates variability in the abundance of exploited species. Nature 443, 859–862.

ICCAT, 2016. Report of the Standing Committee on Research and Statistics (SCRS). pp. 1–426.

Incardona, J.P., Gardner, L.D., Linbo, T.L., Brown, T.L., Esbaugh, A.J., Mager, E.M., Stieglitz, J.D., French, B.L., Labenia, J.S., Laetz, J.S., Tagal, M., Sloan, C.A., Elizur, A., Benetti, D.D., Grosell, M., Block, B.A., Scholz, N.L., 2014. Deepwater Horizon *crude* oil impacts the developing hearts of large predatory pelagic fish. Proc. Natl Acad. Sci. U. S. A 111, E1510–E1518.

Ingram, G.W.Jr., Alvarez-Berastegui, D., Reglero, P., Balbín, R., García, A., Alemany, F., 2017. Incorporation of habitat information in the development of indices of larval bluefin tuna (*Thunnus thynnus*) in the western Mediterranean Sea (2001–2013). Deep Sea Res. Part II: Top. Stud. Oceanogr. 140, 203–211.

Job, S.D., Bellwood, D.R., 2000. Light sensitivity in larval fishes: implications for vertical zonation in the pelagic zone. Limnol. Oceanogr. 45, 362–371.

Juan-Jordá, M.J., Mosqueira, I., Cooper, A.B., Freire, J., Dulvy, N.K., 2011. Global population trajectories of tunas and their relatives. Proc. Natl. Acad. Sci. U. S. A. 108, 20650–20655.

Kim, Y.S., Delgado, D.I., Cano, I.A., Sawada, S., 2015. Effect of temperature and salinity on hatching and survival of yellowfin tuna *Thunnus albacares*. Fish. Sci. 81, 891–897.

Lamkin, J., 1997. The Loop Current and the abundance of larval *Cubiceps pauciradiatus* (Pisces: nomeidae) in the Gulf of Mexico: evidence for physical and biological interaction. Fish. Bull. 95, 250–266.

Lamkin, J., Muhling, B., Lyczkowski-Shultz, J., Ingram, W., Malca, E., Zapfe, G., Gerard, T., Millett, A., Privoznik, S., 2015. Developing new early life history-based fishery independent indices for western atlantic Bluefin tuna. Collect. Vol. Sci. Pap ICCAT 71, 1238–1246.

Lang, K.L., Grimes, C.B., Shaw, R.F., 1994. VVariations in the age and growth of yellowfin tuna larvae, *Thunnus albacares*, collected about the Mississippi River plume. Env. Biol. Fish. 39, 259–270.

Lehodey, P., Chai, F., Hampton, J., 2003. Modelling climate-related variability of tuna populations from a coupled ocean–biogeochemical-populations dynamics model. Fish. Oceanogr. 12, 483–494.

Lindo-Atichati, D., Bringas, F., Gon, G., Muhling, B., Muller-Karger, F.E., Habtes, S., 2012. Varying mesoscale structures influence larval fish distribution in the northern Gulf of Mexico. Mar. Ecol. Progr. Ser. 463, 245–257.

Lindo-Atichati, D., Bringas, F., Gon, G., 2013. Loop Current excursions and ring detachments during 1993–2009. Int. J. Remote. Sens. 34, 5042–5053.

Llopiz, J.K., Richardson, D., Shiroza, A., Smith, S., Cowen, R., 2010. Distinctions in the diets and distributions of larval tunas and the important role of appendicularians. Limnol. Oceanogr. 55, 983–996.

Lohrenz, S.E., Fahnenstiel, G.L., Redalje, D.J., Lang, G.A., Chen, X., Dagg, M.J., 1997. Variations in primary production of northern Gulf of Mexico continental shelf waters linked to nutrient inputs from the Mississippi River. Mar. Ecol. Prog. Ser. 155, 45–54.

Loose, L.L., Dawidowicz, P., 1994. Trade-offs in diel vertical migration by zooplankton: the costs of predator avoidance. Ecology 75, 2255–2263.

Majkowski, J., 2007. Global fishery resources of tuna and tuna-like species. FAO Fisheries Technical Paper 54 FAO, Rome (No 483).

Margulies, D., 1993. Assessment of the nutritional condition of larval and early juvenile tuna and Spanish mackerel (Pisces: scombridae) in the Panama Bight. Mar. Biol. 115, 317–330.

Maunder, M.N., Sibert, J.R., Fonteneau, A., Hampton, J., Kleiber, P., Harley, S.J., 2006. Interpreting catch per unit effort data to assess the status of individual stocks and communities. ICES J. Mar. Sci. 63, 1373–1386.

Muhling, B., Lamkin, J.T., Roffer, M.A., 2010. Predicting the occurrence of Atlantic bluefin tuna (*Thunnus thynnus*) larvae in the northern Gulf of Mexico: building a classification model from archival data. Fish. Oceanogr. 19, 526–539.

Muhling, B.A., Reglero, P., Ciannelli, L., Alvarez-Berastegui, D., Alemany, F., Lamkin, J.T., Roffer, M.A., 2013. Comparison between environmental characteristics of larval bluefin tuna *Thunnus thynnus* habitat in the Gulf of Mexico and western Mediterranean Sea. Mar. Ecol. Prog. Ser. 486, 257–276.

Muller-Karger, F.E., Smith, J.P., Werner, S., Roffer Chen, R., Roffer, R., Liu, Y., Muhling, B., Lindo-Atichati, D., Lamkin, J., Cerdeira-Estrada, S., Enfield, D.B., 2015. Natural variability of surface oceanographic conditions in the offshore Gulf of Mexico. Prog. Oceanogr. 134, 54–76.

Annual commercial fisheries landings statistics, area Gulf, 2016. (Available) https://www.st. nmfs.noaa.gov/commercial-fisheries/commercial-landings/annual-landings.

R Development Core Teamm, 2015. R: a language and environment for statistical computing. R Foundation for Statistical Computing. R Development Core Team, Vienna, Austria. www.R-project.org.

Reglero, P., Tittensor, D.P., Alvarez-Berastegui, D., Aparicio-Gonzalez, A., Worm, B., 2014. Worldwide distributions of tuna larvae: revisiting hypotheses on environmental requirements for spawning habitats. Mar. Ecol. Prog. Ser. 501, 207–224.

Richards, W.J., 2006. Scombridae: mackerels and tunas. Early stages of Atlantic fishes: an identification guide for the western central North Atlantic. CRC, Boca Raton, pp. 2187–2227.

Richardson, D.E., Llopiz, J.K., Guigand, C.M., Cowen, R.K., 2010. Larval assemblages of large and medium-sized pelagic species in the Straits of Florida. Progr. Oceanogr. 86, 8–20.

Roberts, J.J., Best, B.D., Dunn, D.C., 2010. Treml E. A. and Halpin P. N., Marine Geospatial Ecology Tools: An integrated framework for ecological geoprocessing with ArcGIS, Python, R, MATLAB, and C++. Env. Model Soft 25, 1197–1207.

Rooker, J.R., Simms, J.R., Wells, R.J.D., Holt, S.A., Holt, G.J., Graves, J.E., Furey, N.B., 2012. Distribution and habitat associations of billfish and swordfish larvae across mesoscale features in the Gulf of Mexico. PLoS One 7, e34180.

Rooker, J., Kitchens, L.L., Dance, M.A., Wells, R.D., Falterman, B., Cornic, M., 2013. Spatial, temporal, and habitat-related variation in abundance of pelagic fishes in the Gulf of Mexico: potential implications of the Deepwater Horizon oil spill. PLoS One 10, e76080.

Rouyer, T., Fromentin, J.M., Ménard, F., Cazelles, B., Briand, K., Pianet, R., Planque, B., Stenseth, N.C., 2008. Complex interplays among population dynamics, environmental forcing, and exploitation in fisheries. Proc. Natl Acad. Sci. U. S. A 105,

5420–5425.
Satoh, K., Tanaka, Y., Masujima, M., Okazaki, M., Kato, Y., Shono, H., Suzuki, K., 2013. Relationship between the growth and survival of larval Pacific bluefin tuna, *Thunnus orientalis*. Mar. Biol. 160, 691–702.
Scott, G.P., Turner, S.C., Grimes, C.B., Richards, W.J., Brothers, E.B., 1993. Indices of larval bluefin tuna, *Thunnus thynnus*, abundance in the Gulf of Mexico: modeling variability in growth, mortality, and gear selectivity: ichthyoplankton methods for estimating fish biomass. Bull. Mar. Sci. 53, 912–929.
Spinelli, M., Derisio, C., Martos, P., Pájaro, M., Esnal, G., Mianzán, H., Capitanio, F., 2015. Diel vertical distribution of the larvacean *Oikopleura dioica* in a North Patagonian tidal frontal system (42°–45°S) of the SW Atlantic Ocean. Mar. Biol. Res. 11, 633–643.
Tanaka, Y., Satoh, K., Iwahashi, M., Yamada, H., 2006. Growth-dependent recruitment of Pacific bluefin tuna *Thunnus orientalis* in the northwestern Pacific Ocean. Mar. Ecol. Prog. Ser. 319, 225–235.
Taylor, N.G., McAllister, M.K., Lawson, G.L., Carruthers, T., Block, B.A., 2011. Atlantic Bluefin Tuna: A Novel Multistock Spatial Model for Assessing Population Biomass. PLoS One 6, e27693.
Werner, F.E., Mackenzie, B.R., Perry, R.I., Lough, R.G., Naimie, C.E., Blanton, B.O., Quinlan, J., 2001. Larval trophodynamics, turbulence, and drift on Georges Bank: a sensitivity analysis of cod and haddock. Sci. Mar. 65, 99–115.
Wexler, J.B., Chow, S., Wakabayashi, T., Nohara, K., Margulies, D., 2007. Temporal variation in growth of yellowfin tuna (*Thunnus albacares*) larvae in the Panama Bight, 1990–97. Fish. Bull. 105, 1–18.
Wexler, J.B., Margulies, S.M., Sholey, V.P., 2011. Temperature and dissolved oxygen requirements for survival of yellowfin tuna, *Thunnus albacares*, larvae. J. Exp. Mar. Biol. Ecol. 404, 63–72.
Wobbrock, J.O., Findlater, L., Gergle, D., Higgins, J.J., 2011. The Aligned Rank Transform for nonparametric factorial analyses using only ANOVA procedures. In: Proceedings of the ACM Conference on Human Factors in Computing Systems (CHI '11). New York. pp. 143–146.